Proceedings of 20th International Congress on Acoustics, ICA 2010

23–27 August 2010, Sydney, Australia

Fine structures in hearing thresholds and distortion product otoacoustic emissions

Dorte Hammershøi, Rodrigo Ordoñez, Marina Torrente, Felix Kochendörfer

Acoustics, Department of Electronic Systems, Aalborg University, Fredrik Bajers Vej 7 B5, 9220 Aalborg Ø

PACS: 43.64.Jb

ABSTRACT

Otoacoustic emissions (OAEs) are weak sounds that can be recorded in the external ear. They are generated by the active amplification of the outer hair cells, and by many, are considered to reflect the status of the most vulnerable part of the hearing better than ordinary behavioral thresholds. Distortion product OAEs (DPOAES) are generated in response to a two-tone external stimulus with frequencies f_1 and f_2. One of the strongest DPOAEs is the component at $2f_1 - f_2$. This component is elicited on the basilar membrane in the overlap region between f_1 and f_2, close to the f_2 place (depending on frequency ratio and levels of the two-tone stimulus). The $2f_1 - f_2$ component travels along the basilar membrane and excites activity at the $2f_1 - f_2$ place, which yields a second component with the same frequency. The resulting sound that can be recorded in the external ear canal is the superposition of these two components. The result is characterized by a distinct fine structure pattern, and generally does not directly reflect the status of the hearing at one point on the basilar membrane. The behavioral threshold, on the other hand, is more directly related to given points along the basilar membrane, but reflects the combined status of outer and inner hair cells. Thus the combination of DPOAE measurements and hearing thresholds has the potential to provide better basis for hearing diagnosis. In the present study, both DPOAE measurements and hearing thresholds are determined with a fine frequency resolution. The results confirmed that fine structures can be found in both sets of measurements for the group of 12 otologically normal subjects. The DPOAE fine structure is more pronounced than the threshold fine structure, but the width of the two types of fine structure ripples are comparable.

INTRODUCTION

In the human hearing system, the cochlea plays a major role in the cognition of sound. Along its Basilar Membrane (BM), the Outer Hair Cells (OHC) act as an mechanical amplifier for the Inner Hair Cells (IHC), which transform the vibrations into the neural impulses transmitted to the brain. Due to the active process of the OHC, low signals are amplified providing the necessary stimulation needed by the IHC at absolute hearing threshold levels. However, the OHC are also the most sensitive to damage caused by noise. Therefore, direct monitoring of OHC status is an attractive and objective diagnostic tool, when combined with traditional behavioral thresholds.

The active process of the outer hair cells also causes emissions of sound from the cochlea, known as OtoAcoustic Emissions (OAE). These can be spontaneous (SOAEs), or stimulus evoked; by either transients (TEOAEs), clicks (CEOAEs), by continuous stimulus frequency (SFOAEs), or by distortion products (DPOAEs). DPOAEs are excited by two sinusoidal components called primary frequencies f_1 and f_2, characterized by a frequency ratio $f_1/f_2 < 1$ and a level ratio $L_1/L_2 \geq 1$. Two sinusoids with these properties excite several Distortion Products (DP) of which $f_{dp} = 2f_1 - f_2$ is the strongest. This gives DPOAE interesting frequency selectivity characteristics, making the method particularly attractive.

Both in thresholds and in the various OAEs, distinct fine structure patterns can be revealed, if measured with a sufficiently high frequency resolution (i.e Heise et al. 2008, Reuter and Hammershøi 2006). The most immediate explanation for these is the existence of minor irregularities along the basilar membrane, e.g., caused by minor damages. But also pristine cochlea show distinct fine structures, and much still remains to be understood and managed in the comparison of thresholds and OAEs and their fine structures.

For the thresholds and most of the OAEs, the explanation is assumed to relate to the constructive and destructive interference of the original incoming wave and it's reflections from the boundaries inside the cochlea, i.e., at the oval window and the apex. For the DPOAEs, a second phenomenon contributes and probably dominates the fine structure characteristics: The distortion component f_{dp}, generated in the overlap region of the BM (between f_1 and f_2), excites a reflection component at the f_{dp} point on the BM, which adds in or out of phase with the distortion component generated by the primaries. Although the explanation of the various fine structures differ, the periodicities are comparable in magnitude.

The purpose of the present study is to collect and compare fine structures in human thresholds and DPOAEs.

METHODS

DPOAE measurements and thresholds with a high frequency resolution were determined for 12 subjects. The DPOAE measurements were carried out using the ILO96 system. High resolution thresholds were determined using a purpose-built system, based on a PC setup and stimulus produced by Sennheiser HDA 200 headphones. The data analysis was carried out in Matlab.

DPOAE method

The level of the distortion product depends strongly on the frequency ratio of the primaries, and on the levels of the primaries. (Gaskill and Brown 1990, Harris et al. 1989, Kemp and Brown

1983, Nielsen et al. 1993) studied the influence of the frequency ratio f_2/f_1 on the DPOAE amplitude. It was concluded that a ratio of $f_2/f_1 = 1.22$ provides generally the largest DPOAE amplitude, and is therefore used in the present study.

The dependence of the levels of the primaries, incl. their susceptibility to traumas has be studied in a number of earlier investigations (Abdala 1996, Dhar et al. 1998, Gaskill and Brown 1990, Hauser and Probst 1991, Probst and Hauser 1990, Rasmussen et al. 1993, Whitehead et al. 1995a;b). At low levels of the primaries, there is no strong dependence of the level difference between f_1 and f_2, but at higher levels, higher DP levels are obtained, if L_1 is higher than L_2. This level dependence may best be understood by considering the basilar membrane vibration patterns: DPOAEs have been proposed to be a result of nonlinear mechanical interaction between the traveling waves of f_1 and f_2 (Kemp 1986). Results from studies involving suppression of DPOAEs suggest that the f_2 region on the basilar membrane plays a dominant role in the generation of DPOAEs (Brown and Kemp 1984, Harris and Glattke 1992, Kummer et al. 1995). Thus, the highest DP level (L_{DP}) should be generated when the primary traveling waves have comparable vibrational amplitudes at the f_2 region. Comparable vibrational amplitudes of the two traveling waves at the f_2 region can only be achieved when L_1 is higher than L_2 because the f_1 characteristic place is apical to that of f_2. The above argument explains the need to have $L_1 > L_2$ in order to generate high L_{DP}.

DPOAE measurements

In the present investigation, measurements of the DPOAE fine structure within a frequency range so that both the f_2 primary and the distortion product frequency f_{dp} cover one octave band centered at 2 kHz (from 1.4 to 2.8 kHz). It was shown in (Reuter and Hammershøi 2006) that the prevalence of the fine structure is stronger and presents more prevalent ripples in the mid frequency frequency range from 1 kHz to 3 kHz.

To screen the DPOAE fine structure within the frequency range chosen, several measurements were required. The DP-gram test of the ILO96 system was set with a micro resolution. This provides measurements within a range of 200 Hz for $f_2 < 3$ kHz and of 400 Hz for $f_2 > 3$ kHz, presenting 17 pairs of primary tones. Hence, 13 concatenated measurements were required to cover the desired frequency range.

Prior to each measurements the program executes a probe check-fit. It uses a click stimulus to measure the frequency response of the ear canal, detecting anomalies in the probe fit. The data from the check-fit is used to balance and normalize the two primary stimulus levels.

The spectrum analysis is performed by the system applying Fast Fourier Transform (FFT) with a 12.2 Hz resolution. The noise is estimated taking the 10 components closest to $2f_1 - f_2$ in the FFT excluding the distortion product itself. The system presents noise levels as two standard deviation measurements of the background noise (Reuter and Hammershøi 2006).

Threshold method

A fast threshold method with high frequency resolution for determination of fine structure characteristics has been proposed and used by Heise et al. (2008). The algorithm described is a fixed-frequency tracking method for threshold fine structure screening based on the level presentation strategy. The algorithm is known as the "FINE Structure Screening (FINESS) algorithm" (Heise et al. 2008), and for the present investigation, has been implemented in Matlab.

The subjects are instructed to press a button for as long as they can hear the probe stimulus and to release it when they the probe stimulus in nor heard. The level of the stimulus decreases while the button is pressed and it increases when it is released. The stimuli consist of 250 ms tones with a stable interval of 200 ms and raised-cosine raise and fall of 25 ms to facilitate detection. There are no silence intervals between the tones presented. The system is calibrated to present levels adjusted to a dB HL scale according to ISO 389-8 (2004).

The presentation level is changed by 0.75 dB for every stimulus presentation giving an attenuation rate of $\pm$ 3 dB/s. The frequency resolution is of 100 point/octave, and are presented in ascending order. With this high frequency resolution no abrupt thresholds changes are expected to occur from one frequency to the next, allowing for one reversal per frequency. Each ascent and descent in level is made at the same frequency, the frequency of the stimulus changes with reversals in attenuation direction (when the button is pressed or released).

Since only one ascent or descent is presented at each frequency, the threshold estimates are expected to be higher than the true threshold for ascending trials, and lower for descending trials, due to the subject's reaction time. Therefore, the threshold values are calculated using a locally weighted quadratic regression with a span of 9 data points as in Heise et al. (2008). In this manner each threshold level calculated includes both ascending and descending estimates.

Figure 1 shows an example of a screened threshold using the FINESS algorithm. In the figure, each of the ascending and descending trials is at a different frequency.

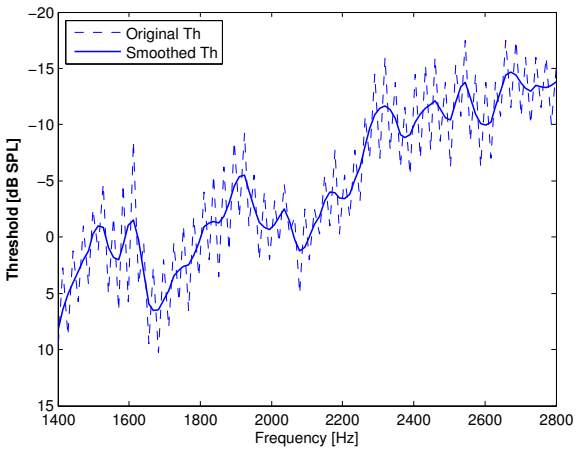

Figure 1: The threshold obtained by the FINESS algorithm (dashed line) is smoothed by applying a locally weighted quadratic regression to calculate the threshold estimate (solid line) with a span of 9 data point.

In (Heise et al. 2008), the repeatability of the FINESS algorithm was tested with a test/retest experiment, and compared to results in an adaptive three-alternative forced choice test. The results showed a high agreement when subjects performed the audiometric test twice. The results also showed a high correlation between the threshold's shape. However, it was also found by a comparison with the 3-AFC method over a wider frequency range, that the thresholds measured with the FINESS algorithm slightly decrease over time as subjects adapt to low level listening. To avoid the effects of adaptation, a familiarization run was performed at the beginning of the measurement. During the familiarization the stimulus frequency is kept constant and several reversals are presented until the difference between consecutive threshold estimates is less than 1.3 dB. A maximum of 16 reversals are presented to ensure that the subject's thresh-

old can be determined to within ± 2 dB of their *asymptotic* threshold (Heise et al. 2008).

Thresholds are determined twice to increase the reliability of the algorithm. In the first run the level of the tone starts decreasing from 50 dB HL, while in the second run the level tracking begins at -20 dB HL and increases until the button is pressed. This gives one ascending and one descending estimate for each frequency.

The consistency between the two thresholds determinations is evaluated at each frequency computing the standard deviation over 11 frequencies of the differences between a normalized threshold estimates given by:

$$T_{norm}(f_i) = w_i \cdot T(f_i) - \frac{1}{n}\sum_{k=1}^{n} w_k \cdot T(f_k), \qquad (1)$$

where $T_{norm}(f_i)$ is the normalized threshold determination at frequency f_i, w is the analysis window of 11 samples centered at the frequency under study. The window consists of 2 samples of raised-cosine raise, 7 flat samples, followed by 2 raised-cosine fall samples.

The threshold determinations are considered to be consistent when the standard deviation of the normalized difference between 11 consecutive normalized threshold determinations (Σ) is less than 2.5 dB. This difference is permitted since this threshold fine structure screening method focuses on the threshold's shape rather than on the level. If the standard deviation is greater that 2.5 dB at one or more frequencies a third threshold determination is conducted at these frequencies.

In the frequency range assessed in the third determination, the two threshold determinations with greatest consistency are found using the standard deviation of the normalized threshold determinations (Equation 1). The threshold obtained in the third repetition is chosen if it is more consistent with either one of the other two determinations. In the limit frequencies of the repeated range the transition is smoothed by cross-fading between the part to be replaced and the threshold determination from the third repetition. An example of a cross-fade between two thresholds measured is illustrated in Figure 2

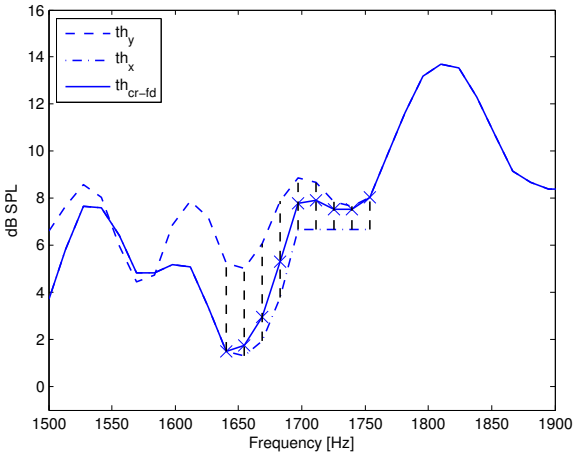

Figure 2: Cross-fading between threshold determinations, shown as a function of frequency. Cross-fading from th_x to th_y is done using Equation 2

The transition points for the cross-fading are calculated as follows:

$$th_{cr-fd} = (1-\alpha)th_x + \alpha \cdot th_y, \qquad (2)$$

where α takes values from 0 to 1 or from 1 to 0, depending on the remeasured frequency limit, in steps of 0.125 giving eight transition steps. th_x correspond to the third repetition of the experiment in an specific frequency range, and th_y is the less consistent of the three repetitions. The cross-fading is applied over the 8 frequencies adjacent to the first and last sample of the frequency interval included in the third repetition.

The final threshold value is calculated as the average between the two resulting curves. Figure 3 shows an example of the entire procedure. The top panel shows the standard deviation of the normalized differences obtained from the data of the first two repetitions. The mid panel shows the threshold determinations for all three repetitions. Finally, the bottom panel shows the two most consistent thresholds, cross-faded in the inconsistent frequency range limits, and the final threshold determination as the average of the corrected curves.

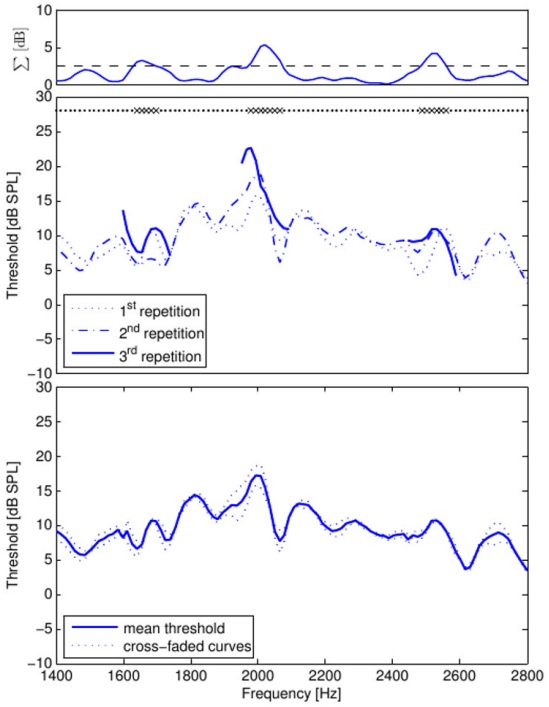

Figure 3: Hearing threshold of a subject measured using the implemented FINESS algorithm. (Top) Consistency check of the first two repetitions and the criteria value of 2.5 dB (dashed line) for the standard deviation of the normalized difference between the threshold determinations (Σ). (Middle) Thresholds obtained from the three repetitions, the solid line shows the thresholds obtained for the third repetition, only at the frequency regions in which the first two determination are inconsistent. (Bottom) The final two determinations constructed from the most consistent threshold from the three repetitions (dotted lines) and the averaged threshold values (solid line).

Threshold measurements

For the present experiment, the frequency range for the threshold measurements is determined by the prevalence of the DPOAE fine structure. A range of one octave centered in 2 kHz is chosen. Thus, the threshold fine structure will be tracked for 100 linearly spaced single frequencies from 1.4 kHz to 2.8 kHz. The time estimated for a single run is of 5 ±1 min.

The FINESS threshold method was implemented in a Matlab program. Sounds were send from the sound card (RME DIGI96/8 PST) of the computer running the experiment to a power amplifier (Pioneer A616), set to a fix gain of 0 dB. The amplified signal was passively attenuated by 40 dB using a resistive circuit attenuating the internal noise from the amplifier

below the hearing threshold. The signal was then fed to a pair of Sennheiser HDA-200 audiometric headphones, placed in the audiometric room together with the response button that was connected to the computer running the experiment. An overview of the audiometric setup is shown in Figure 4

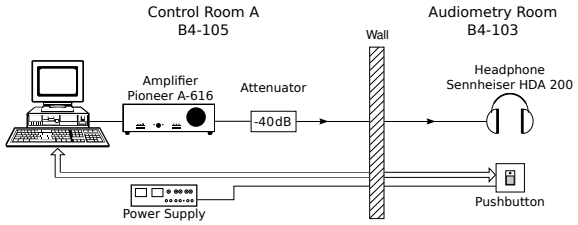

Figure 4: Setup for the FINESS method. To the left is the control room with the computer, amplifier, power supply and attenuator. To the right is the Audiometry room where the subjects were seated equipped with headphones and the response button.

Fine structure classification

The existence of fine structure in hearing threshold or otoacoustic emissions is often determined just by visual inspection. Here, an objective classification of the fine structure is used, which extract the main characteristics of a ripple. These characteristics allow an overall statistical analysis of the measurements, even though the fine structure varies a lot from subject to subject.

The implemented fine structure detector is based on two different algorithms: (Heise et al. 2008) introduced a method for the detection of significant extreme values in threshold fine structure, whereas (Reuter and Hammershøi 2005) developed an algorithm for the classification of DPOAE fine structure.

Each ripple is characterized by its maximum and its two neighboring minima. In order to be accepted as fine structure, adjacent extreme values have to fulfill certain requirements, which need to be specified: The level difference between adjacent minima and maxima should be higher than a minimum level ΔL_{min} and the frequency spacing between the two minima should be in a range between Δf_{min} and Δf_{max}.

In (Reuter and Hammershøi 2006) a ripple spacing between 1/21 and 1/6 octave for DPOAE fine structure was reported, whereas (Heise et al. 2008) proposed a criterion for the spacing of two adjacent extreme values (minimum - maximum) between 1/50 and 1/10 octave. The chosen parameters $\Delta f_{min} = 1/25$-octave and $\Delta f_{max} = 1/5$-octave are based on the proposal by (Heise et al. 2008), and agrees with the observations of (Reuter and Hammershøi 2006).

For DPOAE measurements, a $\Delta L_{min} = 3$ dB was chosen as in (Reuter and Hammershøi 2006), since a high number of low-level variations appear in the measurements. However, threshold measures show in general a lower height of the ripples, but also less fluctuations which are not considered as fine structure. Hence, the minimum level criterion applied for the detection of threshold fine structure is set to $\Delta L_{min} = 2$ dB.

Detection Procedure

The detection of relevant extreme values which characterize a ripple follows an iterative process. Each detection starts at a maximum at f_{max}. All minima within the range $[f_{max} - \Delta f_{max}, f_{max} + \Delta f_{max}]$ which fulfill the criterion of ΔL_{min} are used for further analysis. In the following, minima at frequencies lower than f_{max} will be referred to as 'left' minima (according to its position in the plot regarding the maximum) and minima at frequencies higher than f_{max} as 'right' minima.

Minima which have a greater frequency spacing to f_{max} than the left or right minimum with the lowest level are neglected, since they do not represent an absolute minimum in the range of a ripple. Furthermore, if a minimum is separated from the others by a maximum higher than ΔL_{min}, it is considered to count for a new ripple and to be analyzed separately. Figure 5, shows examples of the ripple detection procedure for threshold and DPOAE ripple determination. Data from two different subjects are used. In the example for the threshold (top panel), the minima and the maximum that leads to the classification of one valid ripple are shown. In the example of the DPOAE (lower panel) the minima and the maximum detected do not fulfill all the required criteria and does not lead to the classification of a valid ripple.

The figure is not meant as a comparison between ripples in thresholds and DPOAEs.

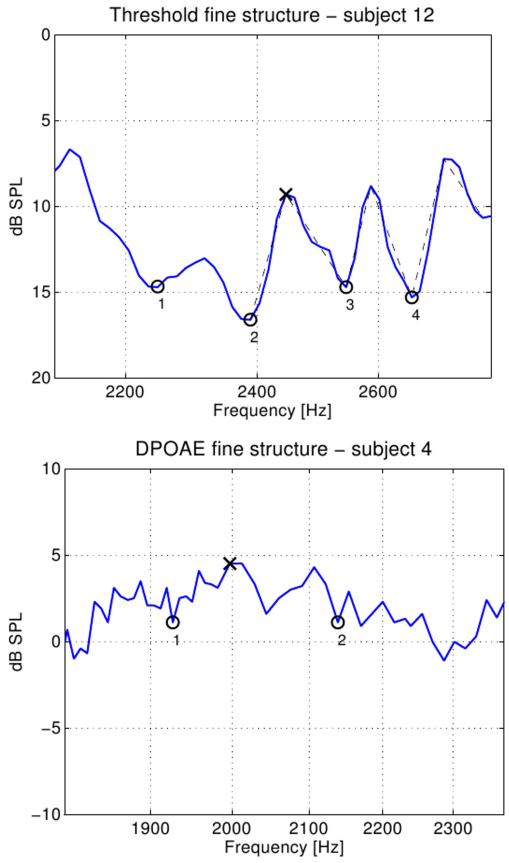

Figure 5: Segments of the threshold curve from subject 12 (above) and DPOAE curve from subject 4 (below). Minima which fulfill the criteria with respect to the maximum (marked with 'X') are indicated by circles. The dashed line in the top panel shows the finally accepted extreme values which characterize the fine structure. For the DPOAE data of the lower panel, the marked maxima and minima do not fulfill all the required criteria, thus are not considered as a ripple.

An example is given in the threshold of subject 12 in the top panel of Figure 5. The 'X' denotes the maximum under current analysis. Minima in the range $[f_{max} - \Delta f_{max}, f_{max} + \Delta f_{max}$ are marked with a circle. Minima 1 and 2 are considered to be left and 3 and 4 right minima. No. 1 is not considered as a possible minimum representing a ripple around f_{max}, because minimum 2 appears at lower level, whereas minimum 4 is neglected because of the maximum between 3 and 4 which may represent separate ripple.

The maximum under analysis is considered as subsidiary and

will therefore be neglected if one of the following cases occur:

- no left or no right minimum is detected
- no pair of left and right minima has a frequency spacing between Δf_{min} and Δf_{max}
- a higher maximum appears between the closest left and right minima, meaning that the current maximum does not represent an absolute maximum in the analyzed range.
- the relation of the frequency spacing of the closest detected minima to the ripple height is higher than $\frac{\Delta f_{max}}{(2\,\Delta L_{min})}$, meaning that the lower the height of the ripple the narrower it has to be.

The latter restriction is due to detections in measurements as a result of low fluctuations and not of real existing fine structure. An example can be seen in the DPOAE measurement of subject 4 in lower panel of Figure 5, where the minima 1 and 2 would fulfill the initial requirement regarding the maximum marked with an 'X', but obviously those extreme values do not represent a ripple.

Once a maximum is neglected the whole procedure continues at the next maximum at a higher frequency.

If the maximum fulfills all requirements, the remaining left and right minima are analyzed further in pairs of all possible combinations. An ideal ripple is considered to have following characteristics:

- the frequency of the maximum is centered between the frequencies of the two adjacent minima
- both adjacent minima have the same level
- the height of the ripple is as high as possible

Hence, the pairs are analyzed regarding those three criteria. The two minima, which are closest to this ideal ripple are accepted and characterize a fine structure ripple together with the current maximum.

Modifications for DPOAE fine structure detection

For the detection of fine structure in DPOAE measurements, the algorithm is slightly modified compared to the threshold fine structure detector. The ILO system also provides measurements of the noise floor, which is represented as the limit of the 95% confidence region. According to the algorithm proposed by (Reuter and Hammershøi 2006), ripples shall be rejected, whenever a maximum is less than 3 dB above the noise floor. However, minima below the noise floor are still regarded for the analysis.

Furthermore ripples in the DPOAE fine structure often appear higher than threshold ripples and show typically very narrow notches characterizing a minimum. Absolute maxima of ripples are not necessarily centered between the two minima, hence the detection of the optimal pairs of minima is weighted more to ripple height than to an equally frequency spacing.

Subjects and procedure

Twelve subjects, 7 males and 5 females, between 20 and 31 years of age participated in the experiment. Two of the subjects suffered from undiagnosed occasional tinnitus. One subject had surgery at the age of 3 and another subject suffered from otitis during his childhood. All thresholds measured by the pure-tone standard audiometry where above 30 dB HL.

The experiment consisted in three tests:

- Standard audiometry
- High resolution audiometry
- DPOAE fine structure measurements

Before starting the experiment the subjects were previously instructed not to come directly from a noisy environment. Thus, at least during half an hour prior to the experiment they should stay in a relaxed and advisable quiet atmosphere.

The subjects were given written and oral instructions before the tests, and had opportunity to ask questions to the procedure and see the test rooms in advance. They were asked to fill in a questionnaire, which addressed their hearing and exposure history.

The first test in the experiment was the standard audiometry. The standard audiometry was conducted to obtain an estimate of the absolute threshold level at a discrete number of frequencies. The test lasted 10 minutes approximately.

The second test was the high resolution audiometry. The aim of this test was to screen the subject's threshold fine structure. The test lasted 20-25 minutes.

The third test was the DPOAE fine structure measurements. This test did not imply the active participation of the subjects, but they were asked to sit still and avoid swallowing. The subjects' DPOAE fine structures were measured with the ILO96 system as described in the preceding section. The test had a duration of 20-30 minutes.

In order to test the repeatability of the implemented high resolution audiometer a subset of 4 subjects (2 males and 2 females) performed the high resolution audiometry test twice. The first repetition was carried out with a at least one week before the retest, which was performed together with the other the standard audiometry and the DPOAE measurements. The reasons for conducting the test/retest threshold screening experiment in different days was entirely practical, maintaining the duration of the main experiment to less than 1 hour and a half. Breaks of 5 minutes were included between the tests in order to ensure comfort and concentration from the subjects.

RESULTS

Individual results

The thresholds, DPOAES and the outcome of the fine structure classification analysis are presented for three subjects in Figures 6, 7, and 8. These examples are more or less randomly chosen, but they represent the variation across subjects fairly.

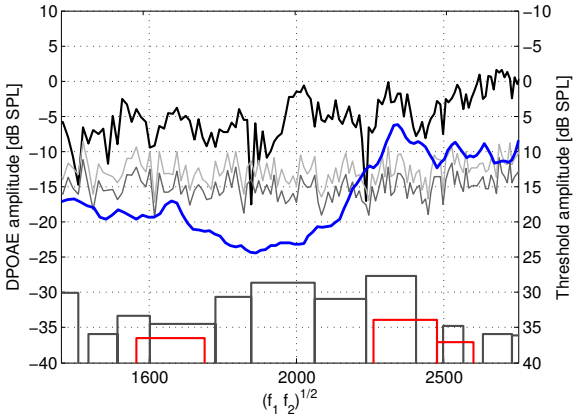

Figure 6: Threshold (blue), threshold fine structure (red), DPOAE (black), DPOAE fine structure (black), and estimates for the DPOAE noise floor (gray) for subject 1. The measured DPOAE level is presented as a function of the geometric mean of the primaries.

The individual results for subject 1 are presented in Figure 6.

Neither threshold nor DPOAE levels are high for this subject, but there are fine structures detected in both the threshold and the DPOAE. For the threshold, the fine structures are not as clear as in the DPOAE. In the DPOAE the fine structures are fairly regular, but the contour also has some micro structures.

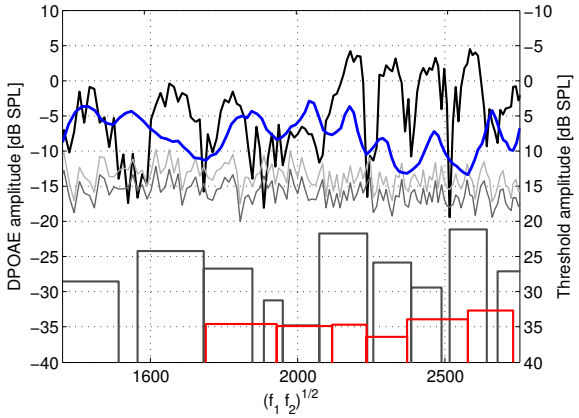

Figure 7: Threshold (blue), threshold fine structure (red), DPOAE (black), DPOAE fine structure (black), and estimates for the DPOAE noise floor (gray) for subject 2. The measured DPOAE level is presented as a function of the geometric mean of the primaries.

Individual results for subject 2 are presented in Figure 7. The DPOAE are slightly higher for this subject than the results presented in Figure 6. Also the fine structures both in threshold and DPOAE are more pronounced. This example also reveals a difference in contour of the two types of fine structures: The DPOAE has the characteristic comb filter shape, which is the most common in transmissions with one distinct, later version of a given first component. The contour of the threshold fine structure, in that the peaks are more defined than the dips, which are more valleys than dips. This is in agreement with models of the threshold, when considering the multiple path environment (Talmadge et al. 1998).

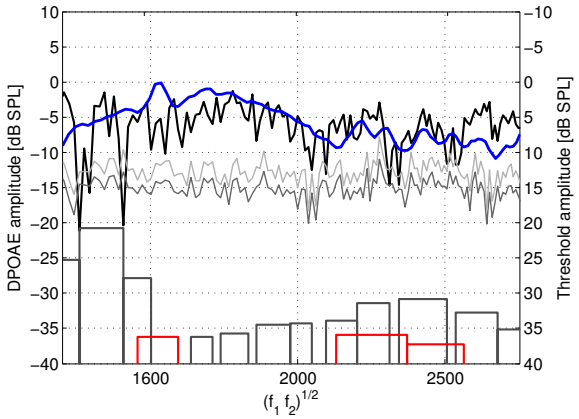

Figure 8: Threshold (blue), threshold fine structure (red), DPOAE (black), DPOAE fine structure (black), and estimates for the DPOAE noise floor (gray) for subject 3. The measured DPOAE level is presented as a function of the geometric mean of the primaries.

The individual result for subject 3 is presented in Figure 8. The threshold show only little fine structure. In this subject, DPOAE fine structures are detected in the full frequency range included. The fine structures have high amplitude in the lowest frequency range, but otherwise are fairly low. A visual inspection may not have lead to the same classification, since the fine structures in this case is also overlaid with micro structures.

An analysis of the prevalence of fine structure ripples, ripple spacing, and ripple height for all subjects are presented in the following.

Ripple prevalence

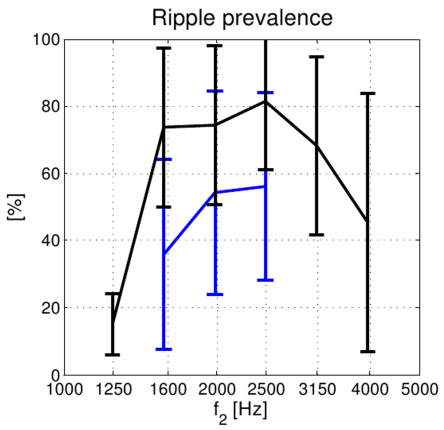

Figure 9: DPOAE (Black) and thresholds (Blue) ripples' prevalence averaged across subjects as a function of 1/8-octave bands. The error bars represent the standard deviation between subjects.

The prevalence of the threshold and DPOAE fine structure ripples are quantified as the percentage of DPOAE or threshold classified as fine structure within a specific frequency range. The average of fine structure ripples prevalence is shown in Figure 9 for all subjects as a function of 1/3-octave bands. It can be seen that the prevalence of DPOAE ripples as a function of f_2 is higher at the mid frequency range centered at 2.5 kHz. Similar results can be found in (Reuter and Hammershøi 2006). The maximum ripples prevalence also appears in the threshold fine structure in the 2.5 kHz band.

When comparing the threshold ripple prevalence curve to the prevalence of DPOAE as a function of frequency the DPOAE prevalence is on average higher than the threshold prevalence over the measured frequency range. This was also the case for the individual results, where the threshold ripple prevalence is always lower than the DPOAE prevalence as a function of frequency. Only subjects 2 and 11 present a prevalence of the threshold ripples higher than 70%. This corresponds in both cases to a presence of DPOAE ripples of 90% or higher within the frequency range from 1.4 to 2.8 kHz.

Ripple spacing

The frequency spacing of the ripples is analyzed in order to establish a possible relationship between the threshold and DPOAE fine structures' periodicity. The analysis of the fine structure ripples' spacing is illustrated in Figures 11 in octaves, and in Figure 10 Hz respectively. The spacing of the fine structure ripples is calculated in 1/8-octave bands for each subject and averaged across subjects.

The threshold ripple's spacing fluctuates around 1/10-octave, with a maximum average spacing of 1/8-octave and a minimum of 1/15-octave. At the lowest frequency the average spacing is 70 Hz and it increases up to 193 Hz on average at higher frequencies. In the literature there is no agreement on the exact periodicity range of the threshold fine structure. It varies from one study to another (Heise et al. 2008).

When analyzing the DPOAE fine structure spacing as a function of $f_{dp} = 2f_1 - f_2$ the average spacing is 1/11-octave with a standard deviation of 1/72-octave. Hence, the spacing increases

from 47 Hz at the lowest frequency to 154 Hz at high frequencies. If the DPOAE ripple's spacing is now analyzed as a function of f_2 the average spacing is also 1/11-octave, with a standard deviation of 1/69-octave. However, this corresponds to a spacing from 68 Hz at the lowest frequency to 255 Hz at high frequencies.

A similar growth is observed in the DPOAE ripple's spacing as a function of frequency when compared to the results presented in (Reuter and Hammershøi 2006). Moreover, this pseudo-linear growth curve appears to be in concordance with the threshold ripple's spacing as a function of frequency.

The frequency spacing of the ripples does however depend on the parameters used by the fine structure detector. When an objective fine structure detector algorithm is designed, it is normally necessary to define some parameters that establish the rules to neglect or accept ripples as fine structure. Those parameters are based in general on a compromise between frequency spacing a level height of the ripples, meaning that specific values of those are already expected. This will influences the variance of the fine structure ripples and could, therefore, be a reason of disagreement among different studies.

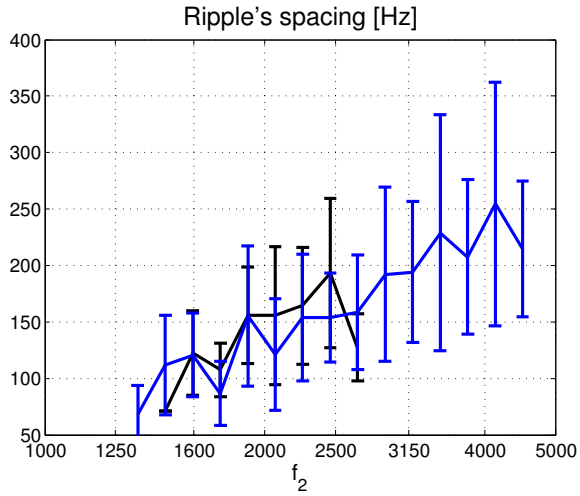

Figure 10: Average across subjects ripple spacing (in Hz) for DPOAE (blue) and thresholds (black) fine structures, as a function of frequency. The error bars represent the standard deviation between subjects.

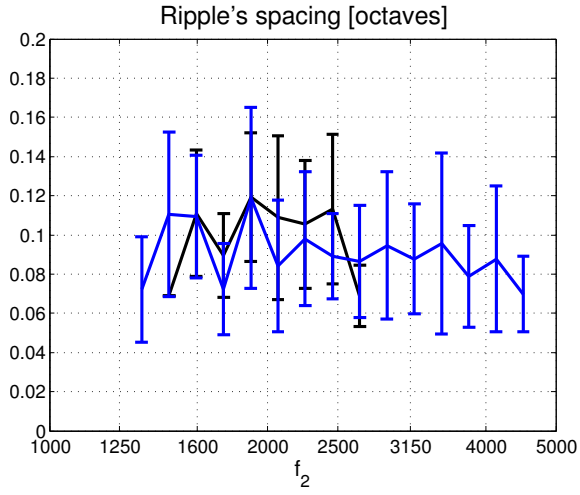

Figure 11: Average across subjects ripple spacing (in octaves) for DPOAE (blue) and thresholds (black) fine structures, as a function of frequency in octaves. The error bars represent the standard deviation between subjects.

Ripple height

The average threshold and DPOAE ripple height are shown in Figure 12 as a function of frequency. The height of the ripples is calculated in 1/8-octave bands and averaged over the 12 subjects.

The threshold ripple height fluctuates around 4.8 dB SPL on average with a standard deviation of 1.4 dB SPL. The height of the DPOAE ripples is on average 8 dB SPL within the analyzed 1/8-octave frequency bands, with a standard deviation of 3.9 dB SPL.

A specific trend as a function of frequency can not be found for the ripple height, both in the case of thresholds and DPOAE fine structures. However, the threshold ripples' height appears lower more constant than the DPOAE ripples' hight.

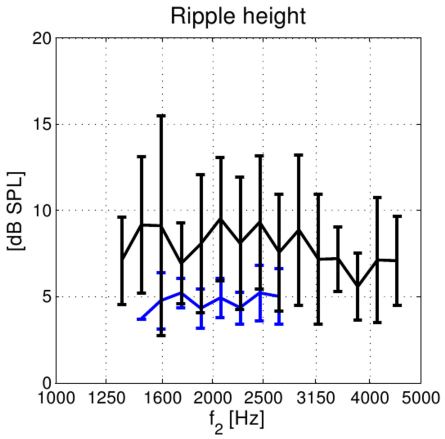

Figure 12: DPOAE (Black) and thresholds (Blue) ripples' height averaged across subjects as a function of 1/8-octave bands. The error bars represent the standard deviation between subjects

DISCUSSION

Measurements of fine structures in DPOAEs and hearing thresholds require high frequency and level resolution to reveal small level differences within a narrow frequency range. Increasing frequency resolution usually leads to a higher measurement time, which is a drawback especially for psychoacoustic measurements such as audiometry, that require full concentration of the subject during the entire test. Therefore, it is necessary to use a method that can probe a large number of frequencies in a short period of time. The implemented audiometer based on the FINESS algorithm satisfies these requirements, but it has certain limitations.

One such limitation is the accuracy with which the method can determine the real absolute threshold level. The FINESS algorithm presents only one tracking at each frequency and it determines the final threshold from several reversals obtained at different frequencies. This is similar to making a running average over a range of peaks and dips, giving a bias to the calculated threshold level at a specific frequency. This approach to the calculation of the threshold and the presentation of probe frequencies in ascending order, relies on the assumption that the threshold values will not present extreme variations from one frequency to the next due to the high frequency resolution.

The purpose of this experiment was to evaluate the height and the periodicity of low level variations of individual thresholds. For this analysis, the absolute threshold level is not as important as the individual shape of the threshold curve. The reliability tests showed a high correlation between the results obtained for the same subjects in different weeks. Additionally, a comparison

of thresholds obtained with the FINESS and the ascending method did not show significant differences. This confirms the validity of the method for the purpose of screening threshold fine structures.

In general, the fine structures reported here, show a good agreement with fine structure data reported by other authors (Heise et al. 2008, Reuter and Hammershøi 2006). However, due to the fine structure detection algorithm, the results can be biased. Since there are no clear definitions for DPOAE or threshold fine structures, the limits of the detection algorithm were adjusted according to previous investigations. Hence, all parameters like ripple spacing, height and prevalence are influenced by initial restrictions for the classification of a ripple.

CONCLUSION

The purpose of the present investigation was to compare DPOAE and threshold fine structures. DPOAEs and thresholds were obtained with a high frequency resolution from 12 subjects and the results were analyzed with an objective ripple detection algorithm. The analysis of the fine structures showed that in the octave band centered at 2 kHz: (1) DPOAE and thresholds have similar ripple spacing of about 0.08 octaves and that they rather stable within the measured octave band. (2) DPOAEs ripples' prevalence and height plotted as a function of f_2 are greater and have similar forms than the prevalence and height of the thresholds fine structure ripples.

These results suggest that there are common elements to the fine structures of DPOAEs and thresholds, specially those related to the fine structure ripple spacing. The greater prevalence and height of the DPOAE ripples also indicates that there are additional mechanisms involved in the generation of the DPOAE fine structure.

REFERENCES

C. Abdala. Distortion product otoacoustic emission (2f(1)-f(2)) amplitude as a function of f(2)/f(1) frequency ratio and primary tone level separation in human adults and neonates. *J. Acoust. Soc. Am.*, 100(6):3726–3740, DEC 1996.

A. M. Brown and D. T. Kemp. Suppressibility of the 2f1-f2 stimulated acoustic emissions in gerbil and man. *Hear. Res.*, 13(1):29–37, 1984.

S. Dhar, G. R. Long, and B. Culpepper. The dependence of the distortion product 2f1-f2 on primary levels in non-impaired human ears. *J. Speech Hear. Res.*, 41(6):1307–1318, 1998.

S. A. Gaskill and A. M. Brown. The behavior of the acoustic distortion product, 2f1-f2, from the human ear and its relation to auditory-sensitivity. *J. Acoust. Soc. Am.*, 88(2): 821–839, AUG 1990.

F. P. Harris and T. J. Glattke. The use of suppression to determine the characteristics of otoacoustic emissions. *Seminars in Hearing*, 13:67–80, 1992.

F. P. Harris, B. L. Lonsbury-Martin, B. B. Stagner, A. C. Coats, and G. K. Martin. Acoustic distortion products in humans - systematic changes in amplitude as a function of f2/f1 ratio. *J. Acoust. Soc. Am.*, 85(1):220–229, JAN 1989.

R. Hauser and R. Probst. The influence of systematic primary-tone level variation l2-l1 on the acoustic distortion product emission 2f1-f2 in normal human ears. *J. Acoust. Soc. Am.*, 89(1):280–286, JAN 1991.

S. J. Heise, J. L. Verhey, and M. Mauermann. Automatic screening and detection of threshold fine structure. *Int. J. Audiol.*, 47(8):520–532, 2008. 28th International Congress of Audiology, Innsbruck, AUSTRIA, SEP 03-07, 2006.

ISO 389-8. Acoustics - reference zero for the calibration of audiometric equipment - part 8: Reference equivalent threshold sound pressure levels for pure tones and circum-aural earphones. Technical report, International Organization for Standardization, Geneva, 2004.

D. T. Kemp. Otoacoustic emissions, traveling waves and cochlear mechanisms. *Hear. Res.*, 22(1-3):95–104, 1986.

D. T. Kemp and A. M. Brown. A comparison of mechanical nonlinearities in the cochleae of man and gerbil from ear canal measurements. In R Klinke and R Hartmann, editors, *Hearing: Physiological Bases and Pscychophysics*, pages 82–88. Springer, 1983.

P. Kummer, T. Janssen, and W. Arnold. Suppression tuning characteristics of the 2 f(1)-f(2) distortion-product otoacoustic emission in humans. *J. Acoust. Soc. Am.*, 98(1):197–210, JUL 1995.

L. H. Nielsen, G. R. Popelka, A. N. Rasmussen, and P. A. Osterhammel. Clinical-significance of probe-tone frequency ratio on distortion-product otoacoustic emissions. *Scand. Audiol.*, 22(3):159–164, 1993.

R. Probst and R. Hauser. Distortion product otoacoustic emissions in normal and hearing-impaired ears. *Am. J. Otolaryngol.*, 11(4):236–243, JUL-AUG 1990.

A. N. Rasmussen, G. R. Popelka, P. A. Osterhammel, and L. H. Nielsen. Clinical-significance of relative probe-tone levels on distortion-product otoacoustic emissions. *Scand. Audiol.*, 22(4):223–229, 1993.

K. Reuter and D. Hammershøi. Distortion product otoacoustic emission fine structure analysis of 50 normal-hearing humans. *J. Acoust. Soc. Am.*, 120(1):270–279, JUL 2006.

R. Reuter and D. Hammershøi. Characterization of dpoae fine structure. *Forum Acusticum, Budapest, Hungary: 4th European Congress on Acoustics.*, pages 233–236, paper nr. 6300, 2005.

C. L. Talmadge, A. Tubis, G. R. Long, and P. Piskorski. Modeling otoacoustic emission and hearing threshold fine structures. *J. Acoust. Soc. Am.*, 104(3, Part 1):1517–1543, SEP 1998.

M. L. Whitehead, M. J. McCoy, B. L. Lonsbury-Martin, and G. K. Martin. Dependence of distortion-product otoacoustic emissions on primary levels in normal and impaired ears .1. effects of decreasing L(2) below L(1). *J. Acoust. Soc. Am.*, 97(4):2346–2358, APR 1995a.

M. L. Whitehead, B. B. Stagner, M. J. McCoy, B. L. Lonsbury-Martin, and G. K. Martin. Dependence of distortion-product otoacoustic emissions on primary levels in normal and impaired ears .2. asymmetry in L(1),L(2) Space. *J. Acoust. Soc. Am.*, 97(4):2359–2377, APR 1995b.